NOAA Technical Memorandum ERL ETL-269

LIDAR CROSS SECTIONS OF LIVE FISH

J.H. Churnside
J.J. Wilson
V.V. Tatarskii

Environmental Technology Laboratory
Boulder, Colorado
June 1996

noaa NATIONAL OCEANIC AND ATMOSPHERIC ADMINISTRATION / Environmental Research Laboratories

NOAA Technical Memorandum ERL ETL-269

LIDAR CROSS SECTIONS OF LIVE FISH

James H. Churnside
James J. Wilson
V.V. Tatarskii

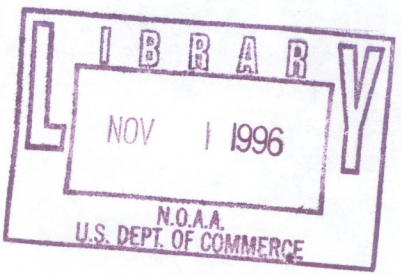

Environmental Technology Laboratory
Boulder, Colorado
June 1996

UNITED STATES DEPARTMENT OF COMMERCE

Michael Kantor
Secretary

NATIONAL OCEANIC AND ATMOSPHERIC ADMINISTRATION

D. JAMES BAKER
Under Secretary for Oceans and Atmosphere/Administrator

Environmental Research Laboratories

James L. Rasmussen
Director

NOTICE

Mention of a commercial company or product does not constitute an endorsement by the NOAA Environmental Research Laboratories. Use of information from this publication concerning proprietary products or the test of such products for publicity or advertising purposes is not authorized.

For sale by the National Technical Information Service, 5285 Port Royal Road
Springfield, VA 22061

Table of Contents

Lidar Cross Sections of Live Fish

James H. Churnside
James J. Wilson
V. V. Tatarskii

NOAA Environmental Technology Laboratory
325 Broadway
Boulder, CO 80303

ABSTRACT: The reflectivity of a school of sardines plus a few anchovies was measured with a polarized lidar operating at a wavelength of 532 nm. The measurements were made in a 10-m-deep tank. The cross-polarization reflectivity was 6.1%, and the co-polarized reflectivity was 19.5%.

1. INTRODUCTION

It was observed in 1981 that fish could be detected using airborne lidar.[1] Several attempts have been made to model the performance of such a system.[2,3] One persistent question in these efforts has been the reflectivity, or the lidar cross section, of fish. Squire and Krumboltz[1] assumed a reflectivity of 50% to estimate the area of the fish intercepted by the lidar. Krekova et al.[2] follow Murphree et al.[3] in assuming a reflectivity of 5%. Fredriksson et al.[4] measured the lidar return from dead fish, but their system was not calibrated. Churnside and McGillivary[5] made calibrated measurements on dead fish and obtained reflectivities of 18-26% for blue and 15-22% for green, depending on species. Benigno and Kemmerer[6] measured the reflectivity of Menhaden in the water at less than 1% across the blue-green portion of the spectrum using natural light.

2. APPARATUS

A block diagram of the lidar system is presented in Figure 1. The laser is a frequency-doubled, Q-switched Nd:YAG laser. The output is linearly polarized, and the laser is equipped with a half-wave plate to rotate the plane of polarization. The beam was diverged and directed to the front of the receiver telescope so that the transmitter and receiver were coaxial. The pertinent transmitter parameters are listed in Table 1. The receiver comprises a refracting telescope that collects the returned signal onto a photo-multiplier tube. An interference filter in front of the detector limits the amount of background light that reaches the detector. A rotatable polarizer in front of the filter allows the co- or cross-polarized return to be selected. The receiver parameters are also listed in Table 1. The photomultiplier output was fed directly into an amplifier with a logarithmic response. The log-amp response is:

$$V_{out} = 0.125\log_{10}(V_{in}) + 0.486, \quad (1)$$

where V_{in} and V_{out} are the input and output voltages.

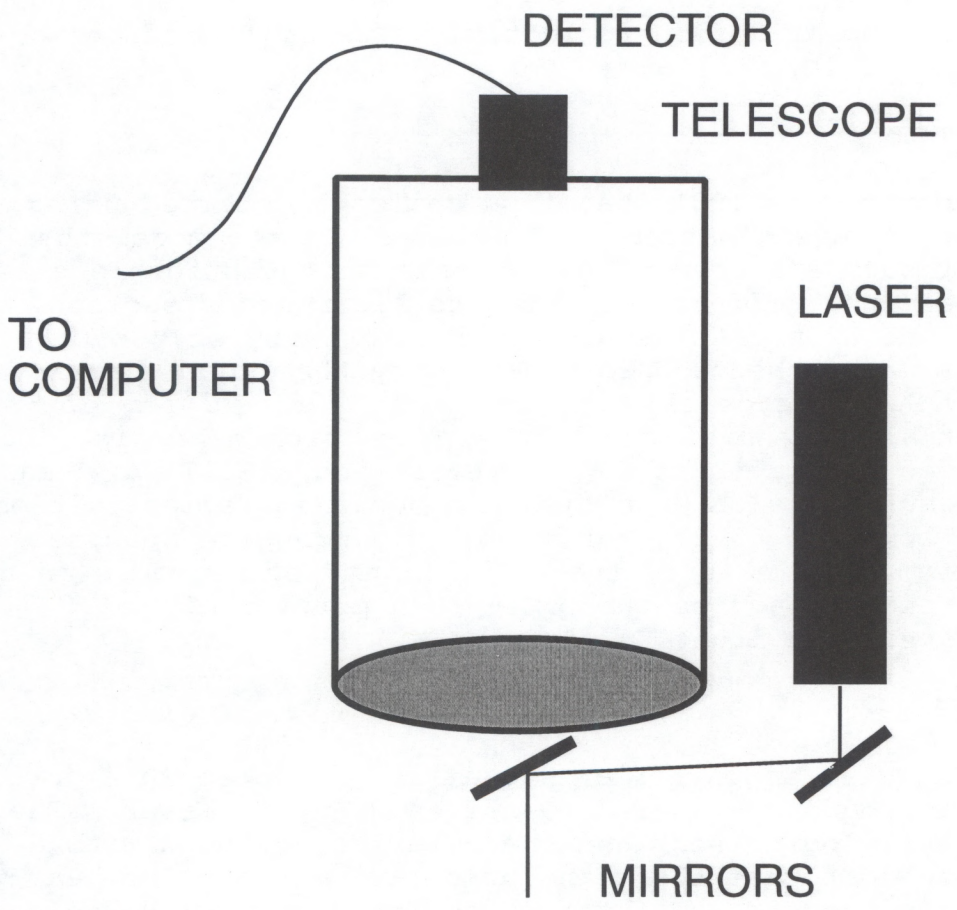

Figure 1. Block diagram of lidar system

Table 1. Parameters of lidar transmitter and receiver.

Transmitter	Wavelength	532 nm
	Pulse Length	15 nsec
	Pulse Energy	67 mJ
	Pulse Repetition Rate	10 Hz
	Beam Divergence	43 mrad
Receiver	Aperture Diameter	17 cm
	Field of View	26 mrad
	Optical Bandwidth	10 nm
	Electronic Bandwidth	300 MHz
	Sample Rate	400 MHz

The log-amp output was digitized with a digital oscilloscope, and the data were transferred to the computer. Because the transfer rate was slow, only one laser pulse in ten could be recorded. Data were recorded in 500-second (i.e., 500 pulses recorded) blocks.

This system was placed on the edge of the deep tank at the Scripps Institute of Oceanography. This tank is about 3 m across and about 10 m deep. The system was pointed toward the center of the bottom of the tank at an angle of about 15° from vertical. The polarization was adjusted to be parallel to the plane of surface reflection. A 30-cm-diameter white disk was suspended just above the bottom of the tank. The laser beam just covered the disk, with an estimated diameter of 32 cm at 10 m. The receiver field of view was slightly larger with a 36-cm diameter.

A video camera was set up outside a window about 2 m from the bottom of the tank. While the laser was operating, the shadows of the fish on the disk were video taped.

Live fish were placed in the tank about two weeks before the experiment to give them time to become accustomed to living in the tank. On the day of the experiment, the tank contained approximately 480 sardines and 65 anchovies. Length and weight

data are summarized in Table 2. The sardines were slightly larger than the anchovies and tended to congregate closer to the surface. The fish did not seem to be affected by the laser beam. They did not try to avoid it and did not become startled when it was turned on, even if they happened to be in the beam.

Table 2. Parameters of the fish in the tank.

Species	Parameter	Mean	Std. Dev.
Sardine	Weight (g)	39.3	7.4
	Standard Length (cm)	14.8	7.6
	Fork Length (cm)	16.0	8.4
	Total Length (cm)	17.7	9.3
Anchovy	Weight (g)	13.1	2.0
	Standard Length (cm)	11.2	6.5
	Fork Length (cm)	12.3	6.6
	Total Length (cm)	13.4	7.1

3. RESULTS

Figure 2 is a plot of a typical lidar return for a cross-polarized receiver. The signal is negative and logarithmic, as described in Eq. (1). The three peaks are caused by the return from the surface, the return from the fish, and the return from the bottom, respectively. Each lidar return was examined. For those containing fish, the depth of the fish return peak, the magnitude of the fish return peak, and the magnitude of the bottom return were recorded. Each of the logarithmic signal strengths was converted to an equivalent linear voltage using Eq. (1).

The video frames corresponding to the lidar shots containing fish were digitized. Figure 3 is a typical video image, showing the time and date information, the illuminated disk, and the shadows of fish. This image corresponds to Figure 2. The disk

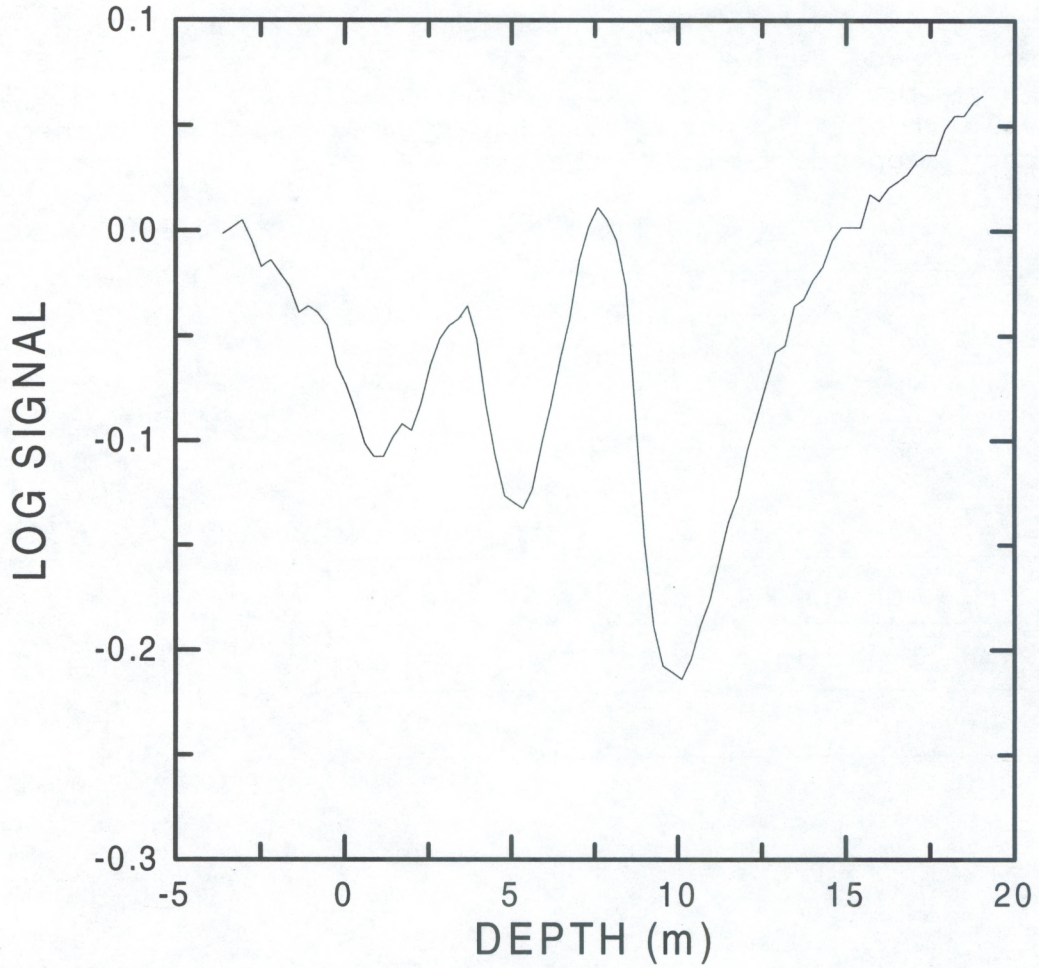

Figure 2. Typical lidar pulse signal with cross-polarized receiver.

appears elliptical because it was recorded from the side. The section of these images containing the disk was selected, transformed to produce a circular image, and thresholded to separate those portions of the disk image that contain fish from those that do not contain fish. An example of the process image of Figure 3 is shown in Figure 4. From these images the fraction of the disk that was covered by fish was found. We represent this fraction by F. For the example shown, F was 29%.

We assume that the lidar return from the disk is proportional to the two-way transmission through the fish school:

$$S_{disk} = C(1-F)^2, \tag{2}$$

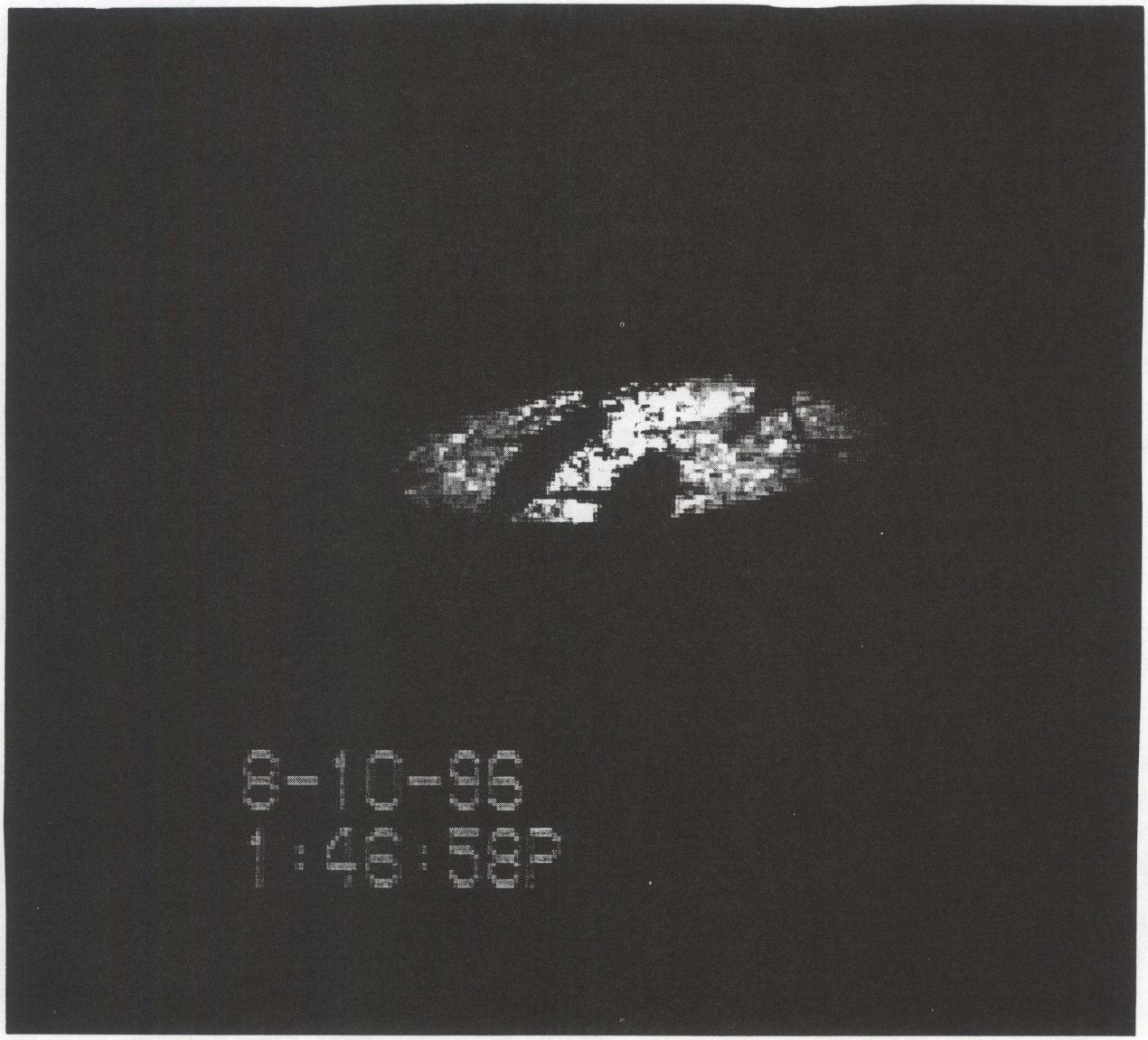

Figure 3. Video image of the fish shadows for the lidar pulse of Fig. 2.

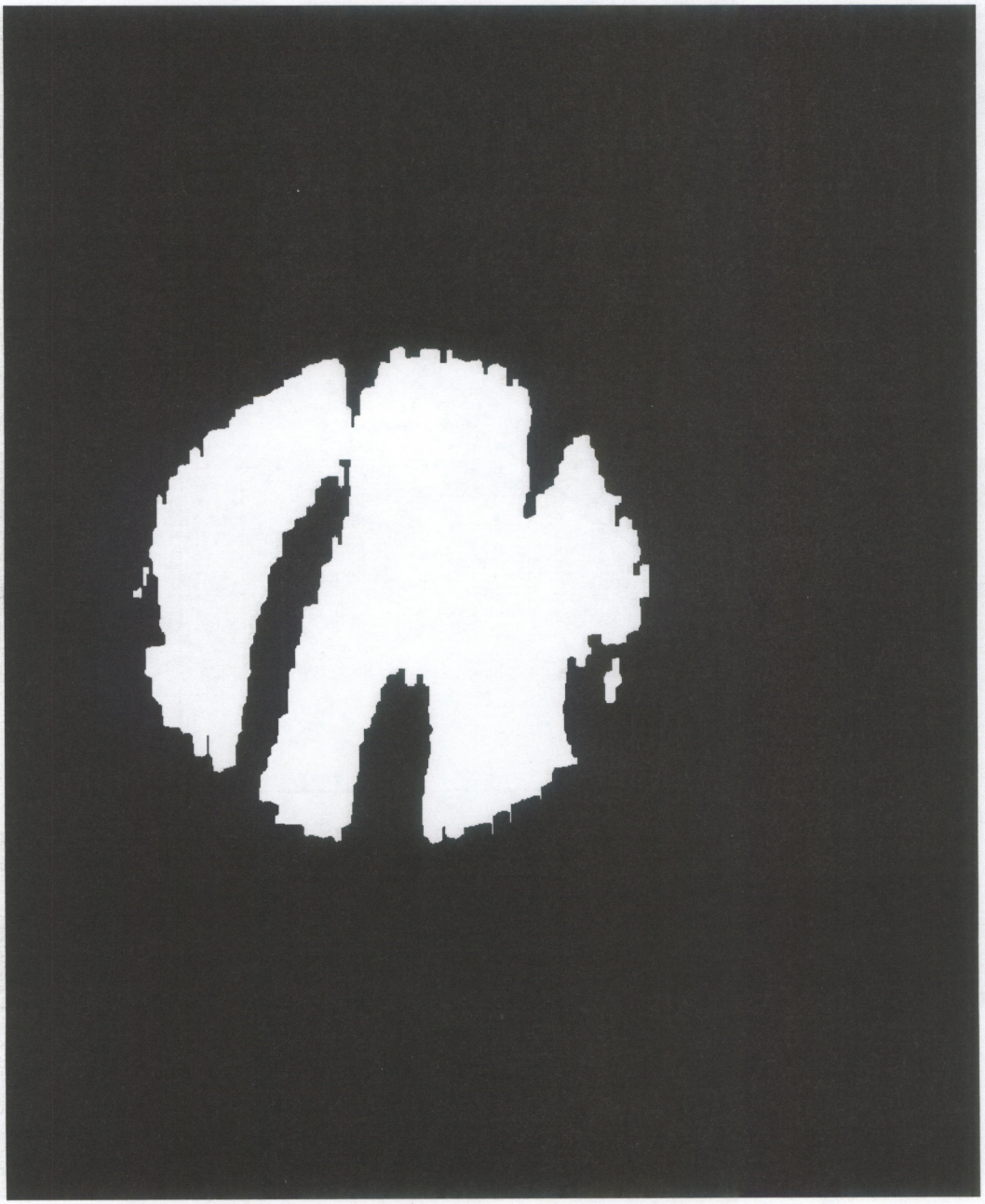

Figure 4. The video image of Fig. 3 after processing.

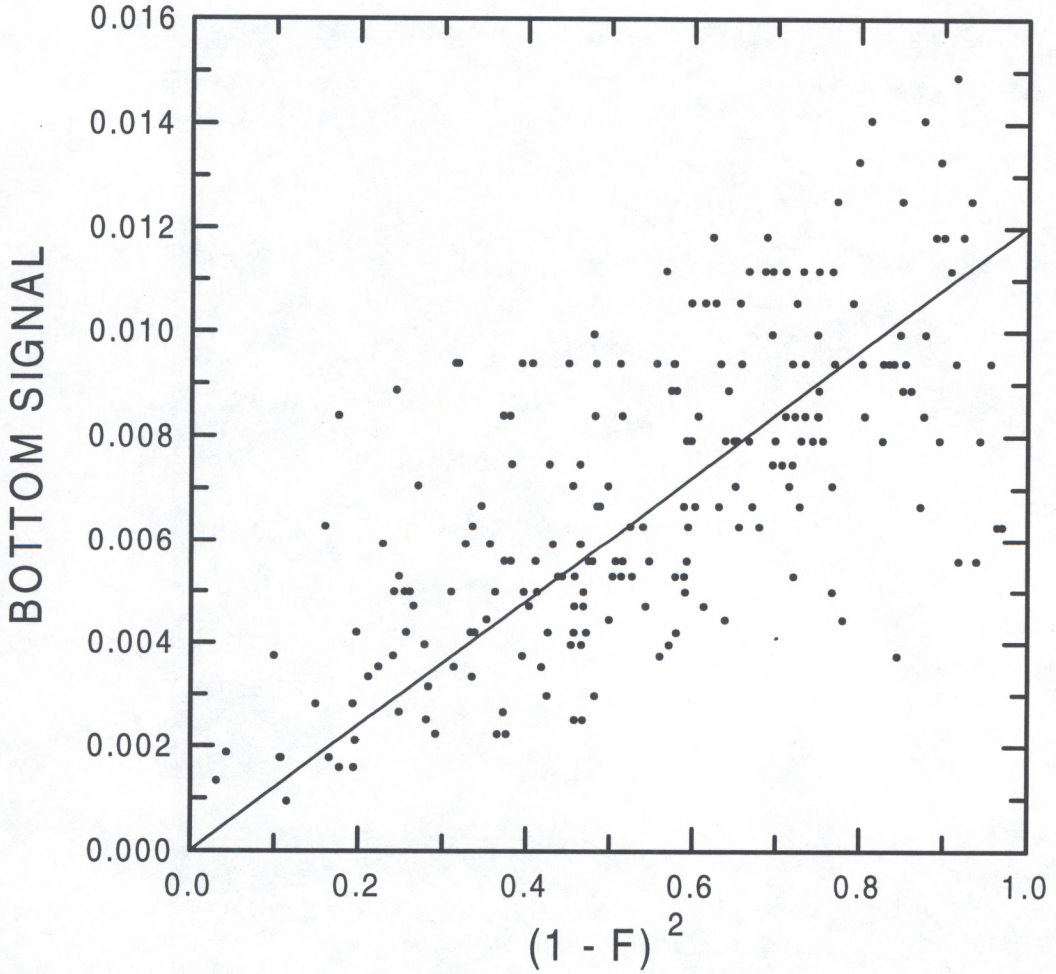

Figure 5. Plot of the magnitude of the bottom return as a function of the round-trip transmission through the school $(1 - F)^{-1}$ for the cross-polarized data. The solid line presents the best linear fit of the data.

where C is a constant to be determined from the data. Figure 5 is a plot of the magnitude of the lidar signal from the bottom for the cross-polarized data set as a function of $(1 - F)^2$. These data include the 210 lidar pulses where there were fish in the beam. Several factors contribute to the scatter in the data by producing variations in the laser irradiance across the beam. These include refraction at the surface and nonuniform scattering by particulates in the water. The solid line in the plot is a linear regression of the data, which provides a value for C of $1.20 \times 10^{-2} \pm 2.71 \times 10^{-4}$.

The signal from the fish can be expressed as:

$$S_{fish} = C\frac{R_{fish}}{R_{disk}}\frac{Z_{disk}^2}{Z_{fish}^2}\exp[-2\alpha(Z_{fish} - Z_{disk})]F, \quad (3)$$

where R represents reflectivity, Z represents depth, and α is the attenuation coefficient of the water. A depth-corrected signal can be defined by

$$S = \frac{Z_{fish}^2}{Z_{disk}^2}\exp[2\alpha(Z_{fish} - Z_{disk})]\, S_{fish}. \quad (4)$$

We use a value of 0.066 m^{-1} for α; with this value there is no residual trend of depth-corrected signal on depth. This value is just above the sea-water absorption coefficient of 0.054 m^{-1} at this wavelength, and is a reasonable value for filtered sea water.

Figure 6 is a plot of the depth-corrected fish signal as a function of F. The linear regression, plotted as the solid line, has a slope of $3.24\times10^{-4} \pm 1.75\times10^{-5}$. Combining these, we have

$$R_{fish} = \frac{3.24\times10^{-4}\pm1.75\times10^{-5}}{1.20\times10^{-2}\pm2.71\times10^{-4}}R_{disk}. \quad (5)$$

The disk used is not Lambertian. We measured its reflectivity in the laboratory at the same angle that was used in the tank. The value was 0.360±0.006 sr^{-1}. Combining all of the uncertainties, we arrive at a value for fish reflectivity of $9.72\times10^{-3} \pm 9.33\times10^{-4}$ sr^{-1}. If we can assume that a school of fish is a Lambertian reflector, we obtain a diffuse reflectivity of 6.1% ± 0.6%.

For the co-polarized data set, there were fewer fish in the beam; only 42 of the lidar pulses contained clear fish returns. Part of the reason for this is that the scatter from the water was much higher in the co-polarized lidar returns, and the fish return

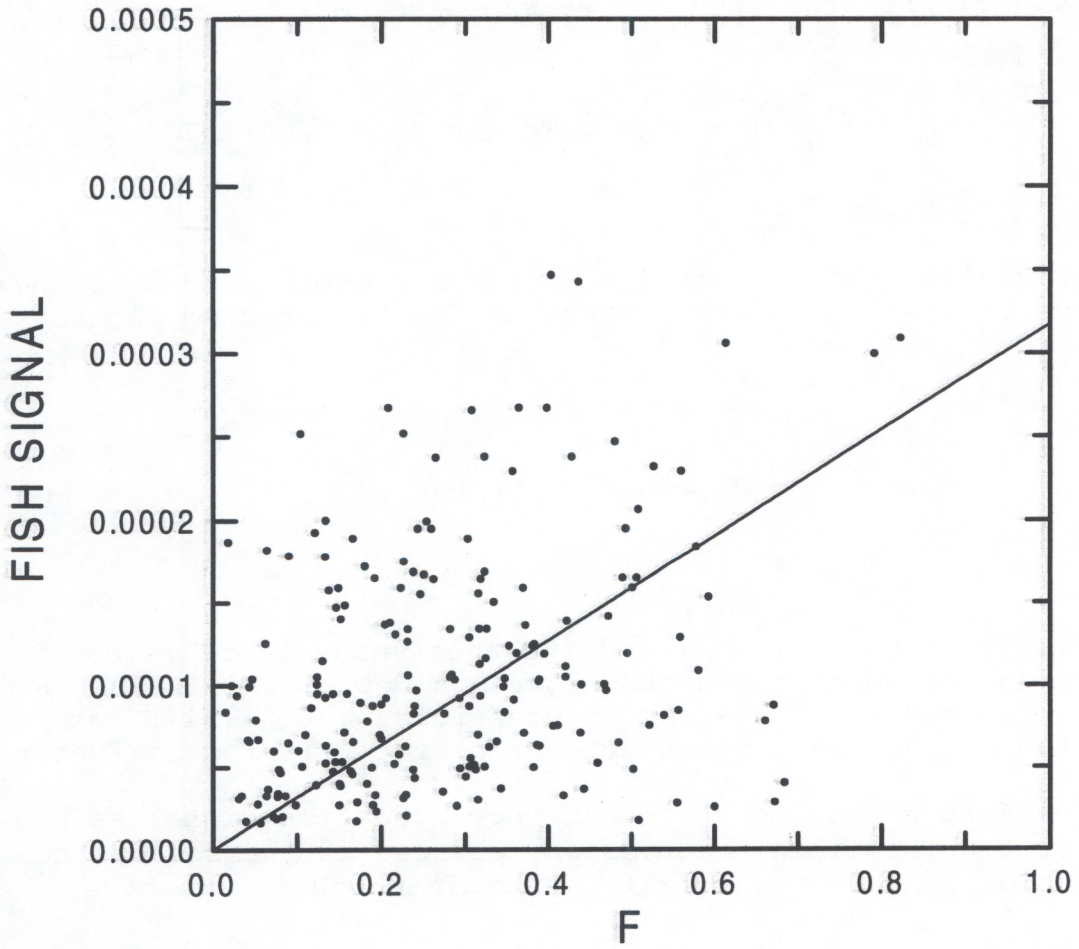

Figure 6. Plot of the depth-corrected fish return as a function of the fraction of the school blocked by fish *F* for the cross-polarized data. The solid line presents the best linear fit of the data.

was more difficult to see. Figure 7 is a plot of the bottom return as a function of $(1-F)^2$ for this data set. The slope of these points, represented by the solid line, is $1.22\times10^{-2} \pm 1.02\times10^{-3}$, which is very close to the value obtained for the cross-polarized data set. We conclude that the measurement is fairly accurate, despite the scatter in the data.

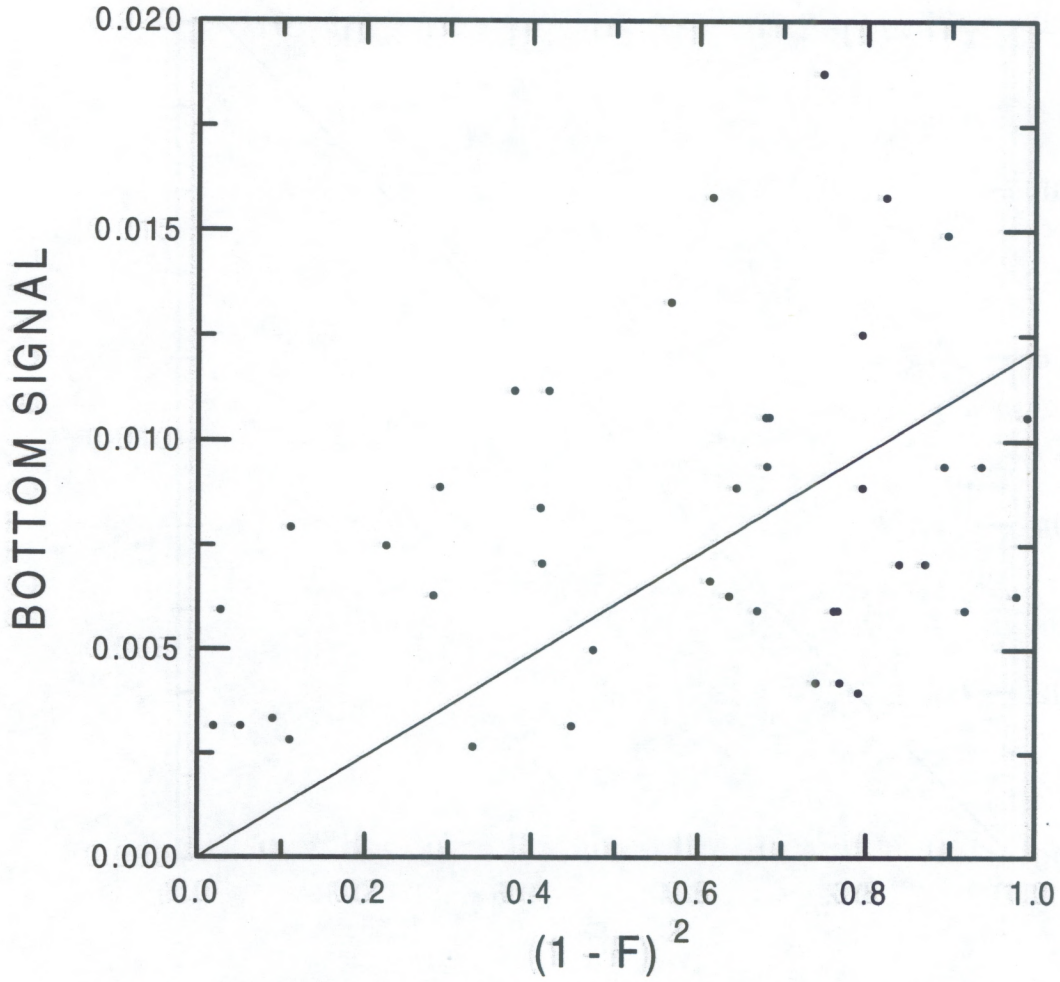

Figure 7. Plot of the magnitude of the bottom return as a function of the round-trip transmission through the school $(1 - F)^2$ for the co-polarized data. The solid line presents the best linear fit of the data.

The fish data were treated as before, and Figure 8 is a plot of the depth-corrected fish signal as a function of F. The slope in this case is $1.05 \times 10^{-3} \pm 1.17 \times 10^{-4}$. The reflectivity is therefore $3.10 \times 10^{-2} \pm 6.54 \times 10^{-3}$ sr^{-1}. The diffuse reflectivity is 19.5% ± 4.1%.

The reflectivity for unpolarized light is the average of the co-polarized and cross-polarized values, or about 13%. This is slightly lower than the range of values measured using dead fish. The depolarization ratio is the ratio of the cross-polarization to the co-polarization, or about 31%. This is within the range of values measured using dead fish.

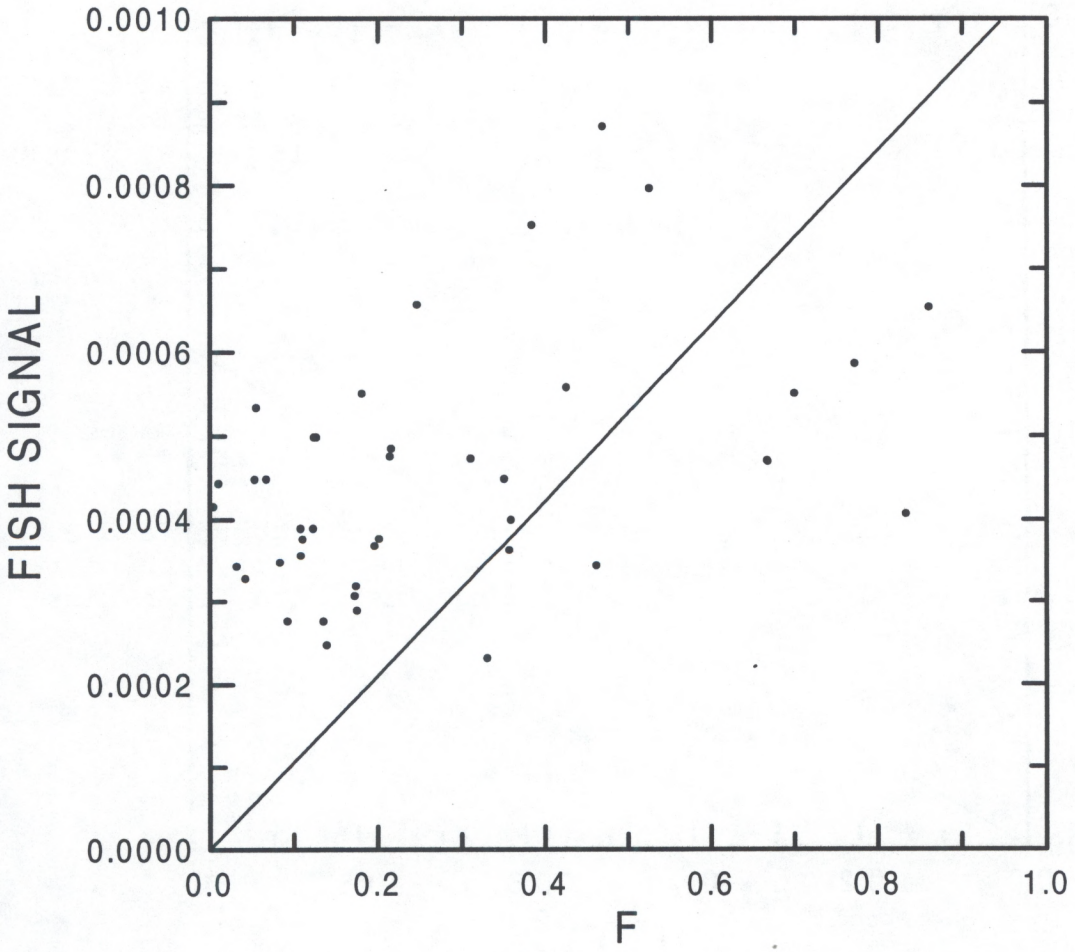

Figure 8. Plot of the depth-corrected fish return as a function of the fraction of the school blocked by fish *F* for the co-polarized data. The solid line presents the best linear fit of the data.

Acknowledgments: This experiment was suggested by John Hunter. Larry Robertson stocked, fed and cared for the fish. Dan Higgens developed programs to process both lidar and video data. This work was partially supported by a joint NOAA/DOD Advanced Sensor Applications Program.

REFERENCES

1. J. L. Squire, Jr. and H. Krumboltz, "Profiling Pelagic Fish Schools Using Airborne Optical Lasers and Other Remote Sensing Techniques," *Mar. Technol. Soc. J.* **15**, 27-31 (1981).

2. M. K. Krekova, G. M. Krekov, I. V. Samokhvalov, and V. S. Shamanaev, "Numerical Evaluation of the Possibilities of Remote Sensing of Fish Schools," *Appl. Opt.* **33**, 5715-5720 (1994).

3. D. L. Murphree, C. D. Taylor, and R. W. McClendon, "Mathematical Modeling for the Detection of Fish by an Airborne Laser," *AIAA J.* **12**, 1686-1692 (1974).

4. K. Fredriksson, B. Galle, K. Nyström, S. Svanberg, and B. Öström, "Underwater Laser-Radar Experiments for Bathymetry and Fish-School Detection," Göteborg Institute of Physics Report GIPR-162 (1978) 28 pp.

5. J. H. Churnside and P. A. McGillivary, "Optical Properties of Several Pacific Fishes," *Appl. Opt.* **30**, 2925-2927 (1991).

6. J. A. Benigno and D. J. Kemmerer, "Aerial Photographic Sensing of Pelagic Fish Schools: A Comparison of Two Films," Proc. ASP Symp. on Remote Sens. in Ocean., Lake Buena Vista, Florida (1973).